Get3 is a holdase chaperone and moves to deposition sites for aggregated proteins when membrane targeting is blocked

Katie Powis[1,6], Bianca Schrul[2,3,6], Heather Tienson[4], Irina Gostimskaya[1], Michal Breker[5], Stephen High[1], Maya Schuldiner[5], Ursula Jakob[4] and Blanche Schwappach[1,2,3,7]

[1] Faculty of Life Sciences, University of Manchester, Michael Smith Building, Oxford Road, Manchester, M13 9PT, UK

[2] Department of Biochemistry I, Faculty of Medicine, University of Göttingen, Humboldtallee 23, 37073 Göttingen, Germany

[3] Max-Planck Institute for Biophysical Chemistry, 37077, Göttingen, Germany

[4] Department of Molecular, Cellular, and Developmental Biology, University of Michigan, Ann Arbor, Michigan 48109, USA

[5] Department of Molecular Genetics, Weizmann Institute of Science, Rehovot, Israel 76100

[6] These authors contributed equally to this work

[7] Author for correspondence (e-mail: blanche.schwappach@med.uni-goettingen.de)

Running title: Cytosolic GET complex in proteostasis

Key words: chaperones, GET pathway, tail-anchored proteins, glucose starvation

JCS online publication date 30 November 2012

SUMMARY

The endomembrane system of yeast contains different tail-anchored proteins that are posttranslationally targeted to membranes via their C-terminal transmembrane domain. This hydrophobic segment may be hazardous in the cytosol if membrane insertion fails resulting in the need for energy-dependent chaperoning and the degradation of aggregated tail-anchored proteins. A cascade of GET proteins cooperates in a conserved pathway to accept newly synthesized tail-anchored proteins from ribosomes and guide them to a receptor at the endoplasmic reticulum where membrane integration takes place. It is, however, unclear how the GET system reacts to conditions of energy depletion that might prevent membrane insertion and hence lead to the accumulation of hydrophobic proteins in the cytosol. Here we show that the ATPase Get3, which accommodates the hydrophobic tail anchor of clients, has a dual function; promoting tail-anchored protein insertion when glucose is abundant and serving as an ATP-independent holdase chaperone during energy depletion. Like the generic chaperones Hsp42, Ssa2, Sis1 and Hsp104, we found that Get3 moves reversibly to deposition sites for protein aggregates, hence supporting the sequestration of tail-anchored proteins under conditions that prevent tail-anchored protein insertion. Our findings support a ubiquitous role for the cytosolic GET complex as a triaging platform involved in cellular proteostasis.

INTRODUCTION

The cytosol of cells is a crowded aqueous solution enclosed by membranes. In this environment, the exposure of strongly hydrophobic molecules is dangerous because it can precipitate the aggregation of proteins that have not yet achieved, or transiently lost, their native state or are terminally misfolded. Different molecular chaperones assist with the shielding, refolding or targeting to degradation of proteins that transiently or inappropriately expose regions of hydrophobicity (Tyedmers et al., 2010; Hartl et al., 2011). In contrast, membrane proteins permanently and appropriately exhibit strongly hydrophobic segments that are eventually embedded in a cellular membrane. Co-translational membrane targeting minimizes the risk for membrane protein aggregation by coupling translation directly to membrane targeting (Shao and Hegde, 2011), however, there are many membrane proteins that are subject to posttranslational targeting, e.g. mitochondrial membrane proteins, substrates of the posttranslational Sec translocon or tail-anchored membrane proteins destined for the secretory pathway. For these proteins, translation is fully completed before they are targeted to the appropriate membrane and their biogenesis involves the transient exposure of nascent transmembrane segments in the cytosol.

Tail-anchored membrane proteins of the secretory pathway use the recently characterized GET machinery (Hegde and Keenan, 2011; Chartron et al., 2012) comprising several cytosolic factors, most prominently the Get3/TRC40 ATPase, and a receptor at the membrane of the endoplasmic reticulum (ER). Extensive biochemical and structural analysis delineated the following steps during tail-anchored protein biogenesis: engaging the tail-anchored protein when it emerges from the ribosome (Get4, Get5, Sgt2), shuttling the tail-anchored protein through the cytosol (Get3) and mediating its release from Get3 into the ER membrane (Get1, Get2). The nucleotide state of Get3 controls its conformation and hence its ability to interact with tail-anchored proteins. Repeated cycles of tail-anchored protein insertion via the GET pathway are coupled to the ATP hydrolysis cycle of the Get3 protein. Studies focusing on the localization of Get3 have visualized Get3-GFP as being localized to the cytosol as well as the ER during mid-logarithmic growth, consistent with its known role in tail-anchored protein insertion. However, in the absence of the ER membrane receptor comprised of Get1 and Get2, the GFP fusion protein accumulates in distinct foci that also contain mislocalized tail-anchored protein

substrates (Schuldiner et al., 2008). Despite the aggregation potential of such precursors that fail to become correctly membrane integrated, the cellular pathways that modulate any resulting toxic species are poorly understood. In order to address the physiological relevance of Get3-positive foci as designated deposition sites for accumulating tail-anchored proteins, we have characterized the localization of Get3-GFP under various forms of cellular stress with the potential to perturb tail-anchored protein membrane integration.

RESULTS

Get3 localizes to foci following glucose depletion

Wild type (wt) cells expressing Get3-GFP from its endogenous promoter were exposed to a variety of stressful conditions including oxidative and reductive challenge or treatment with $CaCl_2$. Amongst these Get3-GFP was only observed in foci under glucose starvation, i.e. after incubation in synthetic complete (SC) medium lacking a carbon source (-D; Fig. 1A). Get3-GFP localization to foci occurred within 60 minutes of glucose withdrawal (Fig. 1B) and reversed shortly after glucose re-addition (Fig. 1C), which led to the re-localization of Get3 into cytosol and perinuclear ER (Fig. 1D). Get3 re-localization into the cytosol also occurred when the synthesis of new proteins was blocked after glucose starvation and before glucose re-addition (Fig. 1E). Steady-state protein levels of Get3-GFP (Fig. 1F) or endogenous Get3 (Fig. 1G) were unaffected by glucose withdrawal or re-addition even in the absence of new protein synthesis, suggesting that Get3 shuttles in and out of the foci as cellular metabolism changes (Wilson et al., 1996; Ashe et al., 2000). Get3-HA behaved indistinguishably from the GFP fusion protein as determined by indirect immunofluorescence (Fig. 1H) excluding GFP-based artifacts. GFP fusions of the GET receptor proteins Get1 and Get2 did not change localization and remained stable under glucose starvation (Fig. 1I and J). Taken together this data suggests a specific response of Get3 to glucose availability.

Formation of Get3-containing foci requires cytosolic Get4 and Get5

Next, we tested whether Get3 entering foci depended on other GET pathway proteins (Fig. 2A and B) such as the two ER membrane receptor proteins Get1 and Get2 (Schuldiner et al., 2008), or the cytosolic GET proteins Get4, Get5 (Jonikas et al., 2009) and Sgt2 (Battle et al., 2010; Chang et al., 2010; Wang et al., 2010; Chartron et al., 2011; Kohl et al., 2011), which are implicated in loading Get3 with tail-anchored protein clients. We found that both, Get4 and Get5, were required for Get3-GFP to enter foci upon glucose withdrawal and that the upstream GET pathway components, GFP-Get5, which was necessary for Get3's redirection to foci under glucose withdrawal (Fig. 2A and B), and Sgt2-GFP, which was not necessary (Fig. 2A and B) but can interact with Get5 (Chang et al., 2010; Wang et al., 2010; Chartron et al., 2011), also accumulated in Get3-positive foci (Fig. 2C). In contrast, absence of the

ER membrane receptor proteins Get1/Get2 substantially increased the number of cells with Get3-GFP-positive foci (Fig. 2A and B), even in the presence of glucose. Since Get4/5 are implicated in substrate loading and Get1/2 are required for substrate release it seems plausible that Get3 is mostly loaded with clients in the foci. Consistent with this notion the number of Get3-GFP-positive foci was reduced to 15% of the number observed under glucose starvation alone when translation was inhibited at the onset of glucose starvation in wt cells (Fig. 2D).

We thus asked whether tail-anchored protein substrates that cannot be inserted co-localize with Get3 in the foci. To impair Get3-dependent membrane targeting and hence create a large population of non-inserted clients we employed a Δ*get1get2* deletion strain (Fig. 2E). Indeed, when we quantified the co-localization of the tail-anchored protein cherry-Sed5, a client of the GET pathway, with Get3-GFP in foci we observed co-localization in medium containing glucose (11% of all foci) that became extensive upon glucose withdrawal (87% of foci; Fig. 2F). In conclusion, Get3 and tail-anchored proteins are found in cytoplasmic foci when membrane integration of the clients is not possible and glucose depletion significantly increases the co-localization.

Ability to hydrolyze ATP determines Get3 localization to foci

Glucose starvation leads to a transient drastic reduction of cellular ATP levels that recover as the cell adapts to the lack of this carbon source (Wilson et al., 1996; Ashe et al., 2000). AMPK kinase is at the center of a major signal transduction pathway that mediates this adaptation. Thus we asked whether deletion of AMPK kinase subunit-encoding genes *SNF1* or *SNF4* affected Get3-GFP localization to foci upon glucose starvation (Fig. 3A). However, Get3-GFP shuttled into and out of the foci in a Δ*snf1* or Δ*snf4* deletion mutant when the cells were glucose-starved and re-exposed to glucose. This indicates that the major pathway of glucose sensing involving Snf1/Snf4 kinase does not regulate Get3-GFP localization to foci.

ATP hydrolysis is required for repeated cycles of tail-anchored protein insertion (Stefanovic and Hegde, 2007; Favaloro et al., 2008). To investigate whether ATP hydrolysis affected localization of Get3 to foci, we employed a $Get3_{D57E}$-GFP mutant variant, which was modeled on a prokaryotic Get3 homologue ArsA with a five-fold lower affinity for Mg^{2+} and a drastically reduced ATPase activity (Zhou and Rosen, 1999). Interestingly, the $Get3_{D57E}$ variant, which has 8.5-fold lower ATPase activity

as compared to wt Get3 (Fig. 3B) but is unaffected in its ability to bind tail-anchored protein clients (Fig. 3C), localized to the foci even in the presence of glucose (Fig. 3D). Similarly, and in contrast to wt Get3-GFP (Fig. 2E and F), co-localization of $Get3_{D57E}$-GFP and the tail-anchored protein cherry-Sed5 in a Δ*get1get2get3* deletion strain was hardly sensitive to glucose availability (Fig. 3E and F). Hence the reduced ability to hydrolyze ATP may direct Get3 to foci or trap it there whereas the interaction with the ER membrane receptor was shown to be unaffected when D57 was mutated (Mariappan et al., 2011). As for wt, Get3 localization to foci was dependent on Get5 (c.f. Fig. 3D and Fig. 2A and B) implying that the mutant $Get3_{D57E}$ enters the same foci as wt Get3 under glucose starvation. These results strongly suggest that the ability to hydrolyze ATP influences the cellular localization of Get3.

Get3-positive foci contain several chaperones and are devoid of membranes or ribosomes

To understand the nature of the foci we performed a thorough co-localization study with markers for a range of cellular structures that are known to be punctate (Fig. 4). Analysis of Get3-GFP-positive foci compared to proteins that label these compartments excluded the following localizations for Get3-GFP under glucose starvation (Fig. 4A): Golgi (Anp1), endosomes (Chc1), prevacuole (Snf7), peroxisomes (Pex3), ER-mitochondrial exchange sites (Mdm34), nucleus-vacuole junction (Nyv1), lipid droplets (Erg6), P bodies (Dcp2), actin patches (Sac6) and autophagosomes (Ape1).

In contrast, when we tested strains expressing GFP fusions of chaperones Hsp42, Hsp104, Sis1, or the Hsp70 homologue Ssa2 we observed clear co-localization with the foci (Fig. 4B). Hsp42 and Hsp104 have been characterized as markers for deposition sites of aggregated proteins (Kaganovich et al., 2008; Liu et al., 2010), in particular under heat stress conditions (Specht et al., 2011). The scaffolding protein Sgt2 (Chang et al., 2010; Wang et al., 2010; Chartron et al., 2011; Kohl et al., 2011) that was present in the foci (Fig. 2C) can interact with both, Hsp70 chaperones and Get3 (via Get5). Hence the cytosolic GET complex may be one component of a larger chaperoning platform sequestering and possibly triaging proteins that expose hydrophobic surfaces.

To obtain better insight into the morphology of the deposition sites, we employed two complementary electron microscopy techniques to visualize Get3-positive foci. First,

we prepared cryo-sections of glucose-starved and chemically fixed Δ*get1get2* cells expressing Get3-GFP (Fig. 5A to C) a strain likely to yield sections with abundant foci (cf. Fig. 2B). We then used anti-GFP immuno-labeling to mark the foci. This analysis revealed electron-dense and hence protein-rich structures devoid of membranes. The foci were sometimes associated with the vacuole (Fig. 5C and E), a characteristic of insoluble protein deposits (IPODs; Kaganovich et al., 2008). Second, we employed high-pressure freezing and Lowicryl-embedding (Fig. 5D to F), which reduced the efficiency of immuno-labeling but revealed the fibrous nature of the foci and demonstrated the exclusion of ribosomes from the deposition sites. Morphologically similar structures were observed in wt cells under glucose-starvation (Fig. 5D and E) and in Δ*get2* cells in the presence of glucose (Fig. 5F). As in Δ*get1* and Δ*get1get2* strains, tail-anchored proteins cannot be delivered to the ER membrane in this background resulting in the cytosolic accumulation and aggregation of tail-anchored protein clients (Schuldiner et al., 2008). In conclusion, Get3, when unable to deliver tail-anchored protein clients to the ER membrane, is consistently recruited to chaperone-rich foci, which are free of membranes or ribosomes and most probably represent deposition sites for aggregated hydrophobic proteins.

Get3 is relevant to cellular chaperoning capacity and exhibits holdase activity

We found that Hsp104-GFP also moved to foci in a Δ*get3* strain in the presence of glucose (Fig. 6A). This implies that the chaperone reacts to the presence of aggregation-prone proteins supporting our finding that the observed foci are deposition sites for protein aggregates. Interestingly, the co-localization of Hsp104-GFP with a tail-anchored protein client, cherry-Sed5, in the foci formed in either Δ*get3* (Fig. 6B) or Δ*get1get2* (Fig. 6C) strains increased substantially upon glucose withdrawal. This indicates tuning of the cellular response to different threats to proteostasis.

Under heat shock, Hsp104 is well established as a factor that associates with protein aggregates at deposition sites (Kaganovich et al., 2008; Liu et al., 2010; Specht et al., 2011). To address the interplay between Hsp104 and Get3 during different forms of proteotoxic stress, we asked whether Get3-GFP was recruited to foci under heat shock (Fig. 6D) and found that, in contrast to Hsp104-GFP, Get3-GFP remained soluble. This implies that Get3 is not involved in sequestering heat-denatured clients to deposition sites. On the other hand Hsp104-GFP was acutely sensitive to the absence

of Get3 (Fig. 6A). Furthermore, Hsp104-GFP co-localized with Get3-RFP upon glucose starvation but moved to distinct Get3-negative foci upon additional heat shock (Fig. 6E). These data suggest that Get3 activity modulates both, the demand for and the capacity of the cell's cytosolic chaperoning activity, when aggregation-prone proteins challenge the biogenesis or function of cytosolic proteins.

Based on the presence of several chaperones in the Get3-positive foci we investigated whether Get3 displays any chaperoning activity itself. We thus purified Get3 and tested its influence on the aggregation of chemically denatured citrate synthase (CS; Fig. 7A and B) or thermally denatured luciferase (Fig. 7C). Get3 was highly efficient in preventing the aggregation of both model clients exhibiting a maximum inhibition of aggregation when present at a four-fold molar excess of Get3-dimers or a two-fold molar excess of Get3-tetramers (Suloway et al., 2011) to CS. The chaperone activity of Get3 was robust when compared to the prokaryotic chaperone Hsp33, which is highly efficient when oxidized. It is of note that addition of either 2 mM ATP or ADP reproducibly reduced the holdase activity of Get3, implying that Get3 acts most efficiently on these clients in the absence of nucleotides (Fig. 7D). This result is fully consistent with our observations involving mutant $Get3_{D57E}$ (Fig. 3) and the hypothesis that the chaperone holdase activity of Get3 becomes relevant under conditions of energy depletion when Get3 is unable to deliver its tail-anchored protein clients to the ER membrane and when the capacity for protein degradation may also be reduced. Intriguingly, Get3 and its mammalian homologue TRC40 have previously been shown to bind tail-anchored protein clients in the absence of nucleotides (Favaloro et al., 2008; Stefer et al., 2011) and this was true for ATP-hydrolysis deficient $Get3_{D57E}$ (Fig. 3B and C). Most holdase chaperones protect cells from the toxic potential of hydrophobic proteins by preventing their aggregation without the requirement of ATP (Eyles and Gierasch, 2010).

Get3 keeps tail-anchored protein clients amenable to degradation

Auld et al. (2006) found the *GET3* gene to be co-regulated with the proteasome consistent with a functional relationship to ubiquitin-dependent protein degradation. We addressed the fate of the tail-anchored protein client after glucose re-addition by monitoring the steady-state levels of cherry-Sed5 and endogenous Sed5 in cycloheximide chase experiments. During glucose starvation Sed5 was stable (Fig. 8A and B). In the absence of tail-anchored protein insertion (Δ*get1get2* and

Δ*get1get2get3* strains; Fig. 8A and B) Sed5 was less stable in the presence of Get3 (Δ*get1get2* strain) upon glucose re-addition. This raises the possibility that chaperoning by Get3 is a prerequisite for efficient degradation when glucose becomes available again. This scenario is further supported by our observation that in the absence of Get3, Get4 or Get5 (Fig. 8C and D), Sed5 remained stable after glucose re-addition consistent with the notion that Get3 keeps the tail-anchored protein client soluble for other factors to act on it.

DISCUSSION

Integrating the results presented here, we propose that the Get3 ATPase has a second cellular function in addition to its well-characterized role as a factor that targets newly synthesized tail-anchored proteins to insertion sites in the ER membrane (Fig. 8E). This second function as a holdase exploits the chaperone capacity of Get3 to bind hydrophobic regions of proteins and becomes relevant under conditions that interfere with the tail-anchored protein insertion cycle and the delivery of short secretory proteins to the translocon (Johnson et al., 2012), either because the ER membrane receptor for Get3 is absent or because cellular energy levels are significantly depleted. Our characterization of Get3 localization under glucose starvation substantially extends the previous observation that Get3 and tail-anchored protein substrates are found in aggregates in cells lacking the GET receptor (Schuldiner et al., 2008): First, the kinetics and reversibility of the process (Fig. 1) and its dependence on other cytosolic GET components (Fig. 2) argue against an uncontrolled aggregation process. Second, even in the absence of the GET receptor, Get3 remains sensitive to glucose starvation, which maximizes its co-localization with a model tail-anchored client (Fig. 2). This glucose sensitivity in subcellular localization is intimately connected to Get3's ability to hydrolyze ATP (Fig. 3) suggesting that Get3 may directly respond to cellular energy status. In support of this hypothesis, we have excluded a major glucose-sensing signal transduction cascade that involves the yeast AMP-activated kinase Snf1/4 as a putative pathway responsible for the glucose-dependent relocalization of Get3 (Fig. 3).

Cellular quality control is aimed at preventing protein aggregation. However, it becomes increasingly clear that cells possess a second line of defense once the factors involved in counteracting aggregation are overwhelmed (Tyedmers et al., 2010). Live-cell imaging has been key to obtaining insight into the cellular strategies by which aggregating proteins are directed to specific deposition sites and hence spatially segregated from processes that they might interfere with (Kaganovich et al., 2008). Subsequent work has shown that different molecular chaperones are targeted to different types of deposition sites in a complex and dynamic pattern (Specht et al., 2011). Two complementary methods of immuno-electron microscopy unequivocally demonstrate the presence of Get3-GFP at protein-dense foci with fibrillar appearance (Fig. 5). The cytosolic GET complex comprising Sgt2, Get4 and Get5, is implicated in transferring nascent tail-anchored protein precursors from the ribosome to Get3.

Because the details of this transfer and loading process are poorly understood it was critical to determine whether ribosomes are present in the Get3-GFP-positive foci observed under glucose starvation. High-pressure freezing allows the detection of ribosomes by electron microscopy and in combination with immunolabelling Get3-GFP, we were able to reveal that ribosomes are absent from Get3-GFP-positive sites (Fig. 5E and F). This result suggests that the cytosolic GET complex is more than a ribosome-associated transfer complex and exerts control over Get3-client complexes even after loading.

At the deposition sites, Get3 strikingly co-localizes with molecular chaperones that can prevent the aggregation of proteins exposing hydrophobic regions and/or reactivate aggregated proteins (Fig. 4B). The dual function of Get3 as a holdase chaperone and a targeting factor for posttranslational membrane integration may enable fast adaptation of the cell once cellular energy status has improved: Precursor proteins can remain associated with Get3 unless they require the activity of another factor present at the deposition site. The organization of various types of chaperones into larger assemblies controlling aggregation-prone proteins implies that clients can be transferred between effector proteins that decide and execute their fate. The problem of sorting hydrophobic clients between different chaperones that recognize precisely this quality – albeit with very different outcomes for the client protein – has previously been recognized and addressed by elegant in vitro assays (Wang et al., 2010; Hegde and Keenan, 2011). However, our study is the first to define the physiological conditions and cellular structures that integrate the capacity of the GET pathway for hydrophobic protein sorting into global cellular proteostasis. Furthermore, our finding that Get3 acts as a holdase chaperone for clients other than tail-anchored proteins (Fig. 7) raises the possibility that this activity can protect other classes of aggregation-prone proteins. Our findings also question the notion that membrane integration is the only fate available to a client protein once it has been sorted into a complex with Get3 (Fig. 8). A broader contribution of Get3 to cellular quality control is strongly supported by the intricate functional relationship between Get3 and the ubiquitin-proteasome system (Auld et al., 2006) and the wider interaction networks formed by GET associated factors such as Sgt2 in yeast and SGTA and Bag6 in mammalian cells (Chang et al., 2010; Leznicki et al., 2010; Mariappan et al., 2010; Wang et al., 2010; Chartron et al., 2011; Hegde and Keenan, 2011; Hessa et al., 2011; Kohl et al., 2011; Chartron et al., 2012; Leznicki and High, 2012).

We have used two model clients, citrate synthase and luciferase, to monitor Get3's ability to prevent protein aggregation upon chemical or thermal denaturation (Fig. 7). Both proteins contain stretches of ca. 20 amino acids that are rich in hydrophobic residues (http://dgpred.cbr.su.se/; Hessa et al., 2007). Whilst these hydrophobic regions will normally be buried in the hydrophobic core of the enzymes and interruptions by polar residues clearly distinguish them from transmembrane segments they will be exposed upon denaturation and might be recognized by Get3. Interestingly, maximal protection of either client from aggregation required at least a four-fold molar excess of Get3 consistent with the idea that higher-order complexes of Get3 are involved in the holdase function. The recent demonstration that a tetramer of an archeal Get3 homologue forms a hydrophobic chamber capable of accommodating a transmembrane segment (Suloway et al., 2011) raises the possibility that the observed holdase activity involves the occlusion of aggregation-prone hydrophobic surfaces in a cage structure formed by a Get3 tetramer. The observed inhibitory effect of adenine nucleotides on the holdase activity (Fig. 7D) is compatible with the intricate structural interplay of the nucleotide-binding domain and the helices involved in forming the hydrophobic binding site of Get3 (Hegde and Keenan, 2011; Chartron et al., 2012). Furthermore, the negative impact of adenine nucleotides on Get3 holdase activity provides an important link to our observations regarding the localization of Get3 in vivo: Get3 changes its localization when cells are glucose-starved or when alteration of a critical residue by sited-directed mutagenesis interferes with its ATPase activity (Fig. 3). Whilst the tail-anchored protein insertion cycle requires ATP hydrolysis, Get3 will be in a position to exert its holdase function under conditions of energy depletion when hydrophobic proteins accumulate.

It has not been rigorously determined how the threat to cellular proteostasis from different classes of aggregation-prone proteins adds up. The heat sensitivity of the *get* mutants (Shen et al., 2003; Metz et al., 2006; Schuldiner et al., 2008) may be explained by the accumulation of membrane protein precursors that jeopardize the capacity of the cell to withstand the load of misfolded proteins caused by heat shock. Our results clarify this point by clearly demonstrating that the chaperone Hsp104-GFP senses the presence of cytosolically accumulating tail-anchored protein precursors (Fig. 6) and that its localization with respect to clients and Get3 depends on the precise nature of the proteotoxic stress. In conclusion we show that the capacity of Get3 to shield hydrophobic proteins is integrated into a spatially controlled and

intricately regulated network of activities that probe, retain, reactivate or degrade hydrophobic clients. The possibilities for sorting clients between these individual activities are only beginning to emerge.

MATERIALS AND METHODS

Molecular biology and strains

Table S1 lists all the strains, Table S2 all plasmids and Table S3 all oligonucleotides used in this study. General molecular biology and basic yeast methodology followed protocols provided by Ausubel et al. (1997). p415MET25 mCherry-Sed5 (pAA1307) was constructed by fusing the mCherry ORF to the 5′ end of the SED5 ORF via an engineered NotI site coding for three alanines, which was cloned into p415MET25.

Growth conditions

Cells were diluted to an OD600 of 0.2 from an overnight pre-culture and grown to mid-log phase (OD600 of 0.6) in synthetic complete medium (SC). Cells were then harvested by low speed centrifugation, washed twice, and resuspended in SC or medium lacking glucose (SC-D).

Live cell imaging

Images of live cells were acquired at room temperature on a Delta Vision RT (Applied Precision) restoration microscope using a 100x/0.35-1.5 Uplan Apo objective and specific band pass filter sets for FITC or RD-TR-PE. The images were collected using a Coolsnap HQ (Photometrics) camera and representative images from several independent experiments are shown as the results.

Western blotting of total cellular protein extracts

Whole cell lysates were prepared by harvesting 2 ml of culture, treated as indicated, by low speed centrifugation. The pellet was resuspended in 0.1M NaOH and incubated at room temperature for 10 minutes (Yaffe and Schatz, 1984). Samples were then harvested and resuspended in non-reducing SDS-PAGE loading buffer. 10µl of each sample (equivalent of 0.01 OD_{600} unit per lane) was resolved by SDS-PAGE and transferred to nitrocellulose membrane. For protein detection the following antibodies were used: anti-Get3 guinea pig antiserum (Metz et al., 2006), anti-GFP mouse monoclonal B-2 (Santa Cruz), anti-Sed5 antiserum (Schuldiner et al., 2008) and anti-Pgk1 mouse monoclonal 22C5 (Molecular Probes, Invitrogen) followed by either anti-guinea pig-HRP or anti-mouse-HRP conjugated secondary antibodies (Jackson Immunoresearch). Membranes were washed between antibody incubations

in blocking solution (1xTBS, 5% milk powder, 0.02% IGEPAL CA-630) and visualized using a 1:1 mixture of enhanced chemiluminescence (ECL) western blotting reagents (Thermo Scientific). Alternatively, IRDye-conjugated secondary anti-guinea pig, anti-rabbit or anti-mouse antibodies (Li-Cor) were used and visualized employing an Odyssey SA (Figs. 8, S2).

Where indicated, translation was inhibited by the addition of cycloheximide to mid-log cells incubated in SC or SC-D for 1h at a final concentration of 0.5 mM from a stock solution of 50 mM cycloheximide in DMSO. Samples were taken at the indicated time points before collection of whole cell lysate and analysis by Western blotting as described above.

Transmission Electron Microscopy

Yeast cells were grown to mid log phase in SC medium at 30°C as described above and glucose-starved for 1h in SC-D if indicated. For classical immuno-EM, cells were concentrated by filtration and then chemically fixed and processed for cryo-ultrasectioning according to the Tokuyasu method (Tokuyasu, 1973). In detail, concentrated cells in medium were mixed 1:1 with 4% paraformaldehyde/PBS and incubated for 30 min at room temperature. The fixative was replaced by 2% paraformaldehyde/PBS and cells incubated overnight at 4°C. Cells were postfixed for 2h in 4% paraformaldehyde/0.2% glutaraldehyde/PBS on ice and washed three times with 0.02 M glycine/PBS prior to embedding in 10% gelatine. Small blocks were infused with 2.3 M sucrose/PBS at 4°C overnight, mounted on metal pins and frozen in liquid nitrogen. Ultrathin cryo-sections (75 nm) were cut using a cryo-ultramicrotome (Ultracut UCT with EM FCS, Leica) and a diamond knife (Diatome) at -110°C and placed on formvar-coated nickel grids.

For immuno-labeling, sections were incubated with polyclonal rabbit anti-GFP antibodies (Abcam) for 20 min, followed by incubation with protein A-10 nm gold (CMC, Utrecht) for 20 min. Sections were contrasted with 0.4% (w/v) uranyl acetate in 2 M methyl-cellulose for 10 min on ice and embedded in the same solution.

For Lowicryl embedding, cells were grown as described above, rapidly filtered and vitrified using an EM HPM100 (Leica) high-pressure freezer. Fixed cells were further processed by freeze substitution in a Leica EM AFS and embedded in HM20 (Polysciences) according to Kukulski et al. (2011). 75 nm ultrathin sections were cut with an ultramicrotome (Ultracut UCT, Leica), used for immuno-gold labeling

employing antibodies as described above and contrasted with 1% (w/v) uranyl acetate/H_2O for 20 min and lead citrate for 1 min.

All sections were examined with a Philips CM120 transmission electron microscope and micrographs were acquired with a CCD camera (Megaview III, Olympus Soft Imaging Systems). Image processing was performed using iTEM software (Olympus Soft Imaging Systems).

Purification of recombinant proteins

Get3 was expressed in BL21 (DE3) from a pQE80 derivative as a fusion of two Z domains (IgG binding domain of proteinA) to Get3 (Metz et al., 2006). Briefly cultures were grown in autoinduction medium (50 mM NH_4Cl, 25 mM Na_2HPO_4, 25 mM KH_2PO_4, 5 mM Na_2SO_4, 2 mM $MgSO_4$, 0.5% tryptone, 0.25% yeast extract, 0.05% glucose, 0.2% lactose, and 0.5% glycerol supplemented with 200 µg/ml ampicillin) for 22 h. Pelleted cells were lysed by sonification in extraction buffer (50 mM Tris-HCl pH 7.5, 50 mM NaCl, 2 mM Mg-acetate and 1 mM imidazole). Cleared lysates were subjected to ultracentrifugation. Get3 was immobilized on a Ni-NTA column and washed with extraction buffer, eluted with 500 mM imidazole, and dialyzed against TEV cleavage buffer (50 mM Tris-HCl pH 8, 1 mM DTT). After cleavage with TEV protease the Z domain tag and TEV protease were removed by passage over a Ni-NTA column and the Get3-containing flow-through was dialyzed against extraction buffer. For ATPase assays immobilized Get3 ZZ fusion protein was sequentially washed in extraction buffer containing 1% Triton-X100, 1 M NaCl, 5 mM Mg-ATP and 0.5 M Tris-HCl pH 7.5, respectively, in order to remove contaminating ATPases such as prokaryotic chaperones. The protein was eluted with extraction buffer containing 500 mM imidazole and buffer-exchanged on a PD-10 column into the same buffer without imidazole. Sec61β was purified as described in (Leznicki et al., 2010).

ATPase assay

The ATP-hydrolysis rates of Get3 and Get3 D57E (uncleaved fusions to two Z domains) were measured with an NADH-coupled ATP-regenerating system at 25°C. The reaction medium consisted of 50 mM Tris-HCl pH 8.0, 100 mM NaCl, 10 mM

$MgCl_2$, 2 mM phosphoenolpyruvate, 25 units/ml of pyruvate kinase and lactate dehydrogenase, 2 mM ATP, 200 µM NADH and 120 µg/ml Get3.

Sec61β binding assay

Binding of recombinant Get3 protein (uncleaved fusions to two Z domains) to immobilized Sec61β was tested as described in (Leznicki et al., 2010): Sec61β with and without the tail-anchor segment was immobilised on Ultra Link Biosupport beads according to manufactures instructions. 1 µl of 0.5 mg/ml Get3 wt or D57E was added to 50 µl of beads resuspended in 50 mM Tris-HCl, pH 7.5. Binding reactions were allowed to proceed at 4°C for 1 h with constant agitation. Beads were washed 3 times with 50 mM Tris-HCl, pH 7.5, 50 mM NaCl and the bound fractions eluted during 30 min incubation at 37°C in SDS sample buffer. Unbound and bound fractions were analysed by non-reducing SDS-PAGE and Western-blotting.

Chaperone assays

Chaperone assays were performed as previously described (Buchner et al., 1998). Briefly, 12 µM citrate synthase (Roche) was denatured overnight at room temperature in 4.5 M Guanidinium-HCl, 40 mM Hepes pH 7.5. Aggregation was initiated by addition of 75 nM citrate synthase to 40 mM Hepes pH 7.5 at 30°C with or without purified Get3 at the indicated concentrations relative to citrate synthase. Light scattering was monitored at 360 nm in a Hitachi F4500 fluorescence spectrophotometer. Where indicated 2 mM ATP or ADP was added to Get3 and incubated for 1 minute prior to addition of citrate synthase.

Aggregation of Luciferase was initiated by the addition of 120 nM Luciferase to 40 mM Mops pH 7.5, 50 mM KCl at 43°C, with or without the indicated concentrations of Get3. Aggregation was monitored for 900 sec as described in the text.

ACKNOWLEDGEMENTS

We thank P. March (FLS Bioimaging Facility) for support with live cell imaging and D. Riedel, D. Wenzel and G. Heim for technical advice regarding electron microscopy; A. Clancy for expert help with microscopy; P. Leznicki for generously providing purified Sec61β; W. Voth for a control experiment using the chaperone assay; Y. Elbaz, J. Metz and V. Schmidt for the construction of yeast strains; M. Ashe and J. Weissman for generously sharing yeast strains and Schwappach lab members for critical reading of the manuscript. This work was supported by a Wellcome Trust SRF award to B. Schwappach; a British Council BIRAX grant to M. Schuldiner and B. Schwappach; a European Union FP7 Marie Curie reintegration grant (239224) to M. Schuldiner; a National Institute of Aging grant (AG027349) to U. Jakob; a Ralph Kohn fellowship to K. Powis, and by a postdoctoral fellowship from the National Institute of Aging NIA Training Grant (AG000114) to H. Tienson. Author contributions: K.P., Bi.S., M.S., and B.S. designed research; K.P., Bi.S., H.T., I.G., and M.B. performed research; K.P., Bi.S., H.T., I.G., S.H., M.S., U.J., and B.S. analyzed data; S.H., M.S., U.J. and B.S. wrote the paper.

REFERENCES

Ashe, M. P., De Long, S. K. and Sachs, A. B. (2000). Glucose depletion rapidly inhibits translation initiation in yeast. *Mol Biol Cell* **11**, 833-848.

Auld, K. L., Hitchcock, A. L., Doherty, H. K., Frietze, S., Huang, L. S. and Silver, P. A. (2006). The conserved ATPase Get3/Arr4 modulates the activity of membrane-associated proteins in Saccharomyces cerevisiae. *Genetics* **174**, 215-227.

Ausubel, F. M., Brent, R., Kingston, R. E., Moore, D. D., Seidman, J. G., Smith, J. A. and Struhl, K. (1997). Current protocols in molecular biology. New York: Published by Greene Pub. Associates and Wiley-Interscience : J. Wiley.

Battle, A., Jonikas, M. C., Walter, P., Weissman, J. S. and Koller, D. (2010). Automated identification of pathways from quantitative genetic interaction data. *Mol Syst Biol* **6**, 379.

Buchner, J., Grallert, H. and Jakob, U. (1998). Analysis of chaperone function using citrate synthase as nonnative substrate protein. *Methods Enzymol* **290**, 323-338.

Campbell, R. E., Tour, O., Palmer, A. E., Steinbach, P. A., Baird, G. S., Zacharias, D. A. and Tsien, R. Y. (2002). A monomeric red fluorescent protein. *Proc Natl Acad Sci U S A* **99**, 7877-7882.

Chang, Y. W., Chuang, Y. C., Ho, Y. C., Cheng, M. Y., Sun, Y. J., Hsiao, C. D. and Wang, C. (2010). Crystal structure of Get4-Get5 complex and its interactions with Sgt2, Get3, and Ydj1. *J Biol Chem* **285**, 9962-9970.

Chartron, J. W., Gonzalez, G. M. and Clemons, W. M., Jr. (2011). A structural model of the Sgt2 protein and its interactions with chaperones and the Get4/Get5 complex. *J Biol Chem* **286**, 34325-34334.

Chartron, J. W., Clemons, W. M., Jr. and Suloway, C. J. (2012). The complex process of GETting tail-anchored membrane proteins to the ER. *Current Opinion in Structural Biology* **22**, 217-224.

Eyles, S. J. and Gierasch, L. M. (2010). Nature's molecular sponges: small heat shock proteins grow into their chaperone roles. *Proc Natl Acad Sci U S A* **107**, 2727-2728.

Favaloro, V., Spasic, M., Schwappach, B. and Dobberstein, B. (2008). Distinct targeting pathways for the membrane insertion of tail-anchored (TA) proteins. *J Cell Sci* **121**, 1832-1840.

Hartl, F. U., Bracher, A. and Hayer-Hartl, M. (2011). Molecular chaperones in protein folding and proteostasis. *Nature* **475**, 324-332.

Hegde, R. S. and Keenan, R. J. (2011). Tail-anchored membrane protein insertion into the endoplasmic reticulum. *Nat Rev Mol Cell Biol* **12**, 787-798.

Hessa, T., Sharma, A., Mariappan, M., Eshleman, H. D., Gutierrez, E. and Hegde, R. S. (2011). Protein targeting and degradation are coupled for elimination of mislocalized proteins. *Nature* **475**, 394-397.

Hessa, T., Meindl-Beinker, N. M., Bernsel, A., Kim, H., Sato, Y., Lerch-Bader, M., Nilsson, I., White, S. H. and von Heijne, G. (2007). Molecular code for transmembrane-helix recognition by the Sec61 translocon. *Nature* **450**, 1026-1030.

Johnson, N., Vilardi, F., Lang, S., Leznicki, P., Zimmermann, R. and High, S. (2012). TRC-40 can deliver short secretory proteins to the Sec61 translocon. *J Cell Sci* **125**, 3612-3620.

Jonikas, M. C., Collins, S. R., Denic, V., Oh, E., Quan, E. M., Schmid, V., Weibezahn, J., Schwappach, B., Walter, P., Weissman, J. S. et al. (2009).

Comprehensive characterization of genes required for protein folding in the endoplasmic reticulum. *Science* **323**, 1693-1697.
Kaganovich, D., Kopito, R. and Frydman, J. (2008). Misfolded proteins partition between two distinct quality control compartments. *Nature* **454**, 1088-1095.
Kohl, C., Tessarz, P., von der Malsburg, K., Zahn, R., Bukau, B. and Mogk, A. (2011). Cooperative and independent activities of Sgt2 and Get5 in the targeting of tail-anchored proteins. *Biol Chem* **392**, 601-608.
Kukulski, W., Schorb, M., Welsch, S., Picco, A., Kaksonen, M. and Briggs, J. A. (2011). Correlated fluorescence and 3D electron microscopy with high sensitivity and spatial precision. *J Cell Biol* **192**, 111-119.
Leznicki, P., Clancy, A., Schwappach, B. and High, S. (2010). Bat3 promotes the membrane integration of tail-anchored proteins. *J Cell Sci* **123**, 2170-2178.
Leznicki, P. and High, S. (2012). SGTA antagonizes BAG6-mediated protein triage. *Proc Natl Acad Sci U S A* **doi**/10.1073/PNAS.1209997109
Liu, B., Larsson, L., Caballero, A., Hao, X., Oling, D., Grantham, J. and Nystrom, T. (2010). The polarisome is required for segregation and retrograde transport of protein aggregates. *Cell* **140**, 257-267.
Mariappan, M., Mateja, A., Dobosz, M., Bove, E., Hegde, R. S. and Keenan, R. J. (2011). The mechanism of membrane-associated steps in tail-anchored protein insertion. *Nature* **477**, 61-66.
Mariappan, M., Li, X., Stefanovic, S., Sharma, A., Mateja, A., Keenan, R. J. and Hegde, R. S. (2010). A ribosome-associating factor chaperones tail-anchored membrane proteins. *Nature* **466**, 1120-1124.
Metz, J., Wachter, A., Schmidt, B., Bujnicki, J. M. and Schwappach, B. (2006). The yeast Arr4p ATPase binds the chloride transporter Gef1p when copper is available in the cytosol. *J Biol Chem* **281**, 410-417.
Schuldiner, M., Metz, J., Schmid, V., Denic, V., Rakwalska, M., Schmitt, H. D., Schwappach, B. and Weissman, J. S. (2008). The GET complex mediates insertion of tail-anchored proteins into the ER membrane. *Cell* **134**, 634-645.
Shao, S. and Hegde, R. S. (2011). Membrane protein insertion at the endoplasmic reticulum. *Annual Review of Cell and Developmental Biology* **27**, 25-56.
Shen, J., Hsu, C. M., Kang, B. K., Rosen, B. P. and Bhattacharjee, H. (2003). The Saccharomyces cerevisiae Arr4p is involved in metal and heat tolerance. *Biometals* **16**, 369-378.
Specht, S., Miller, S. B., Mogk, A. and Bukau, B. (2011). Hsp42 is required for sequestration of protein aggregates into deposition sites in Saccharomyces cerevisiae. *J Cell Biol* **195**, 617-629.
Stefanovic, S. and Hegde, R. S. (2007). Identification of a targeting factor for posttranslational membrane protein insertion into the ER. *Cell* **128**, 1147-1159.
Stefer, S., Reitz, S., Wang, F., Wild, K., Pang, Y. Y., Schwarz, D., Bomke, J., Hein, C., Lohr, F., Bernhard, F. et al. (2011). Structural basis for tail-anchored membrane protein biogenesis by the Get3-receptor complex. *Science* **333**, 758-762.
Suloway, C. J., Rome, M. E. and Clemons, W. M., Jr. (2011). Tail-anchor targeting by a Get3 tetramer: the structure of an archaeal homologue. *EMBO J*. **31**, 707-719.
Tokuyasu, K. T. (1973). A technique for ultracryotomy of cell suspensions and tissues. *J Cell Biol* **57**, 551-565.
Tyedmers, J., Mogk, A. and Bukau, B. (2010). Cellular strategies for controlling protein aggregation. *Nat Rev Mol Cell Biol* **11**, 777-788.

Wang, F., Brown, E. C., Mak, G., Zhuang, J. and Denic, V. (2010). A chaperone cascade sorts proteins for posttranslational membrane insertion into the endoplasmic reticulum. *Mol Cell* **40**, 159-171.
Wilson, W. A., Hawley, S. A. and Hardie, D. G. (1996). Glucose repression/derepression in budding yeast: SNF1 protein kinase is activated by phosphorylation under derepressing conditions, and this correlates with a high AMP:ATP ratio**.** *Curr Biol* **6**, 1426-1434.
Yaffe, M. P. and Schatz, G. (1984). Two nuclear mutations that block mitochondrial protein import in yeast. *Proc Natl Acad Sci U S A* **81**, 4819-4823.
Zhou, T. and Rosen, B. P. (1999). Asp45 is a Mg2+ ligand in the ArsA ATPase. *J Biol Chem* **274**, 13854-13858.

FIGURE LEGENDS

Fig. 1. Get3 localizes to foci under glucose starvation. (A) Localization time courses of Get3-GFP expressed from the endogenous promoter in the absence of glucose (-D), presence of 200 mM $CaCl_2$, 10 mM DTT and 0.4 mM H_2O_2 over 60 minutes as indicated. Control panel in synthetic complete medium (SC) is shown on the left (cells treated exactly as in the time courses, 60 minute time point). (B) Quantitative analysis of the formation of foci in SC-D (each bar represents 180-300 cells from four colonies in two independent experiments; data shown are the mean ± SD). (C) Quantitative analysis of the disappearance of foci upon the addition of glucose (2% final concentration) to cells previously incubated in SC-D for 60 minutes (each bar represents 110-280 cells from four colonies in two independent experiments; data shown are the mean ± SD). (D) Reversibility of localization of Get3-GFP after exposure of cells that had formed Get3-positive foci to medium containing glucose. The same cells were imaged in an agar pad containing SC after they had been starved for 60 minutes in SC-D in liquid culture. (E) Get3-GFP stability in foci and redistribution to the cytosol are independent of new protein synthesis. Time course of Get3-GFP localization in cells first incubated in SC or SC-D for 60 minutes and then monitored in the presence of 0.5 mM cycloheximide (upper two rows). Time course upon glucose re-addition to 2% final concentration in cells that had been pre-incubated in SC-D for 60 minutes to induce Get3-GFP localization to foci in the presence of 0.5 mM cycloheximide (lower row). (F) Western blot showing steady-state levels of Get3-GFP after glucose starvation and upon re-addition of glucose. (G) Steady-state levels of Get3 in the presence or absence of glucose. After addition of 0.5 mM cycloheximide to inhibit translation cells were incubated in the indicated medium for the indicated time, Western blotting was used to show steady-state levels of Get3. (H) Indirect immunofluorescence detecting Get3-3HA expressed from the endogenous promoter in SC and after 60 minutes of glucose starvation as in (A). Arrows label the perinuclear ER in cells growing in SC and foci in glucose-starved cells. (I) Get1-GFP and Get2-GFP were expressed from their endogenous promoters and were visualised after 60 minutes of incubation in SC and SC-D. (J) Steady-state levels of the indicated GFP fusion proteins in SC or after glucose starvation (60 minutes). (Blots in F, G, J were also probed with an antibody against yeast phosphoglycerate kinase (Pgk1) as a loading control. Scale bars A, D, E, H and I: 5 µm.)

Fig. 2. Get3 localization to foci depends on cytosolic GET components Get4 and Get5 and on the ability of Get3 to deliver clients to the ER membrane. (A) Get3-GFP localization to foci induced by glucose withdrawal (60 minutes; -D) in the indicated strains. Get3-GFP positive foci were not observed in strains lacking either Get4 or Get5. (B) Quantitative analysis of Get3-GFP positive foci in SC and SC-D (each bar represents 200-300 cells from four colonies in two independent experiments; data shown are the mean ± SD). (C) GET pathway components Get5 and Sgt2 co-localize with Get3 in glucose-starvation (60 minutes) induced foci. A strain expressing an N-terminal fusion of GFP to Get5 and a C-terminal fusion to Sgt2 from their endogenous promoters was transformed with a plasmid driving the expression of Get3-tdRFP. (D) Quantitative analysis of the formation of Get3-GFP-positive foci in SC-D in the absence (1% DMSO) or presence of 0.5 mM cycloheximide (CHX; each bar represents 340-420 cells from two independent experiments; data shown are the mean ± SD). (E) Co-localization of tail-anchored protein substrate cherry-Sed5 with Get3-GFP in a strain lacking the ER membrane receptor proteins Get1/Get2, i.e. under conditions where membrane delivery of Sed5 via the GET pathway is impaired (Schuldiner et al., 2008). Cells were imaged in the presence of glucose (SC) and after 60 minutes of glucose withdrawal (-D). (F) Quantification of results obtained from the experiment illustrated with representative images in E. Get3-GFP, cherry-Sed5, or double positive foci were counted in medium containing glucose (SC) or after 60 minutes of glucose withdrawal (-D). (Sale bars A, C and E: 5 µm.)

Fig. 3. A Get3-GFP mutant protein with impaired ATP hydrolysis capacity but intact tail-anchored substrate binding accumulates in foci irrespective of glucose availability. (A) Get3-GFP localization to foci and disappearance from foci upon glucose starvation (-D) or re-addition (-D -> +D) is unaffected by deleting either *SNF1* or *SNF4*, encoding for subunits of AMPK kinase. (B) ATPase activity of wt and D57E Get3 protein (N-terminally tagged with two Z domains). Data shown are the mean of three experiments ± SD. (C) Binding assays demonstrate capacity of $Get3_{D57E}$ (N-terminally tagged with two Z domains) to bind a model tail-anchored protein, Sec61β, via its transmembrane segment with similar efficiency as N-terminally tagged wt Get3. '-TA' indicates construct without transmembrane segment. (D) $Get3_{D57E}$-GFP

accumulates in foci in both, SC and SC-D. While the relocalization of Get3-GFP was independent of glucose availability in the hydrolysis-deficient mutant it depended on the presence of Get5. (E) Co-localization of Get3$_{D57E}$-GFP with tail-anchored protein substrate cherry-Sed5 in a strain lacking the ER membrane receptor proteins Get1/Get2. Cells were imaged in the presence of glucose (SC) and after 60 minutes of glucose withdrawal (-D). (F) Quantification of results obtained from the experiment illustrated with representative images in (E). Get3 $_{D57E}$-GFP, cherry-Sed5, or double positive foci were counted in medium containing glucose (SC) or after 60 minutes of glucose withdrawal (-D). (Scale bars A, D, and E: 5 µm.)

Fig. 4. Several chaperones and the cytosolic GET complex co-localize with Get3 under glucose starvation. (A) Co-localization analysis of Get3-GFP with markers for punctate cellular structures as indicated. Anp1-RFP as a Golgi marker, Chc1-RFP as an endosomal marker, Snf7-RFP as a prevacuolar marker, Pex3-RFP as a peroxisomal marker, Mdm34-RFP as an ERMES marker, Nyv1-RFP as a marker for the nucleus-vacuole junction, Erg6-RFP as a lipid droplet marker, Dcp2-YFP as a P body marker, Sac6-RFP as a marker of actin patches and Ape1-RFP as a marker of autophagosomes were co-localized employing strains expressing both fusion proteins from a genomic copy driven by the endogenous promoter, except for co-localization with Dcp2 where Get3-tdRFP (Campbell et al., 2002) was expressed from a plasmid (c.f. supplementary Tables S1 and S2). (B) Strains expressing C-terminal fusions of GFP to chaperones Hsp42, Hsp104, Sis1, and Ssa2, respectively, from their endogenous promoter were transformed with a plasmid driving the expression of Get3-tdRFP.

Fig. 5. Get3-GFP positive foci are protein-rich, membrane- and ribosome-free deposits. (A to C) Examples of cryosections from glucose-starved and chemically fixed Δ*get1get2* double deletion cells expressing Get3-GFP from its endogenous promoter. Cells were fixed after 60 minutes of glucose withdrawal as in Figure 1. The sections were immuno-labeled with anti-GFP antibody and 10 nm gold particles conjugated to protein A. (White scale bars 200 nm.) (D and E) Sections obtained after high-pressure freezing of glucose-starved (60 minutes) wt cells expressing Get3-GFP from the endogenous promoter. (White scale bars 200 nm; Black scale bar 500 nm.) (F) Example of sections obtained after high-pressure freezing of Δ*get2* deletion cells expressing Get3-GFP from its endogenous promoter without exposing them to

glucose starvation. (White scale bar 200 nm.) ER: endoplasmic reticulum; pnER: perinuclear ER; N: nucleus; V: vacuole; LD: lipid droplet; PM: plasma membrane; CW: cell wall.

Fig. 6. Hsp104-GFP and Get3-GFP react to overlapping yet distinct stress conditions. (A) Localization of Hsp104-GFP in a wt or a Δ*get3* strain in medium containing glucose (SC) or after 60 minutes of glucose withdrawal (-D). (B,C) Quantification of Hsp104-GFP-, cherry-Sed5-, or double positive foci in a Δ*get3* (B) or Δ*get1get2* deletion strain (C) in medium containing glucose (SC) or after 60 minutes of glucose withdrawal (-D). (D) Localization of Get3-GFP or Hsp104-GFP in a wt strain at 30°C or 37°C (heat shock). (E) Co-localization of Hsp104-GFP and Get3-tdRFP in glucose-starved wt cells at 30°C or 37°C (heat shock). Arrow indicates co-localization of the proteins at 30°C. (Scale bars A, D and E: 5 µm.)

Fig. 7. Get3 exhibits holdase chaperone activity that is inhibited in the presence of ATP. (A) Influence of Get3 on the aggregation behaviour of citrate synthase (CS). Chemically denatured CS was diluted 1:160 into buffer in either the absence or presence of increasing amounts of purified Get3. To monitor the aggregation of citrate synthase, light scattering measurements were conducted. Ratios indicate Get3:CS; oxidized Hsp33:CS was 4:1. (B) Aggregation of CS monitored as in (A) in the presence of a 16-fold molar excess of bovine serum albumin (BSA) or Get3. (C) Influence of Get3 on the thermal aggregation of luciferase. Luciferase was diluted 1:100 into 43°C buffer in the absence or presence of increasing concentrations of Get3. Aggregation of Luciferase was monitored by light scattering. Ratios indicate Get3:luciferase; oxidized Hsp33:luciferase was 4:1 (D) Effect of ATP and ADP on the chaperone function of Get3. A two-fold molar excess of Get3 dimer was incubated with or without 2mM ATP or ADP for 1 minute prior to addition of CS. Aggregation of CS in the presence of Get3 alone was set to 100% activity. Data shown are the mean of three experiments ± SD.

Fig. 8. Dual function of the cytosolic GET complex. (A,B) Cells were glucose-starved for 60 minutes, shifted to medium without or with glucose in the presence of cycloheximide (CHX) and monitored by microscopy (A) or Western blot (B) after 30

minutes. Stability of cherry-Sed5 (upper rows of images) or endogenous Sed5 (lower bar diagram summarizing the Sed5 levels relative to Sed5 present before the addition of CHX obtained by Western blot using fluorescent detection; quantification of Sed5 was normalized to Pgk1 levels in the same sample from nine independent experiments ± SE) in wt, Δ*get1get2* or Δ*get1get2get3* deletion strains ($p<0.04$ by student's t-test for the difference between the Δ*get1get2* or Δ*get1get2get3* deletion strains after glucose re-addition). (C,D) Sed5 stability assessed by Western blotting as in (B) in wt or Δ*get3*, Δ*get4*, or Δ*get5* strains at indicated time points after glucose-starved cells were shifted to medium without or with glucose in the presence of CHX; data shown are the mean of three experiments ± SE. (E) Schematic yeast cell illustrating the GET pathway of tail-anchored protein insertion when glucose is available and recruitment of Get3 (labeled '3') to cytosolic deposition sites for aggregated proteins that also contain molecular chaperones such as Hsp70s (labeled '70') and Hsp104 (labeled '104') upon glucose starvation or when Get3 is incapable of hydrolyzing ATP. Numbers '1','2','3','4','5' indicate respective GET components, 'S' labels Sgt2. Dark grey shape represents ribosome and brown shape tail-anchored protein. ER, endoplasmic reticulum, nuc, nucleus, vac, vacuole.

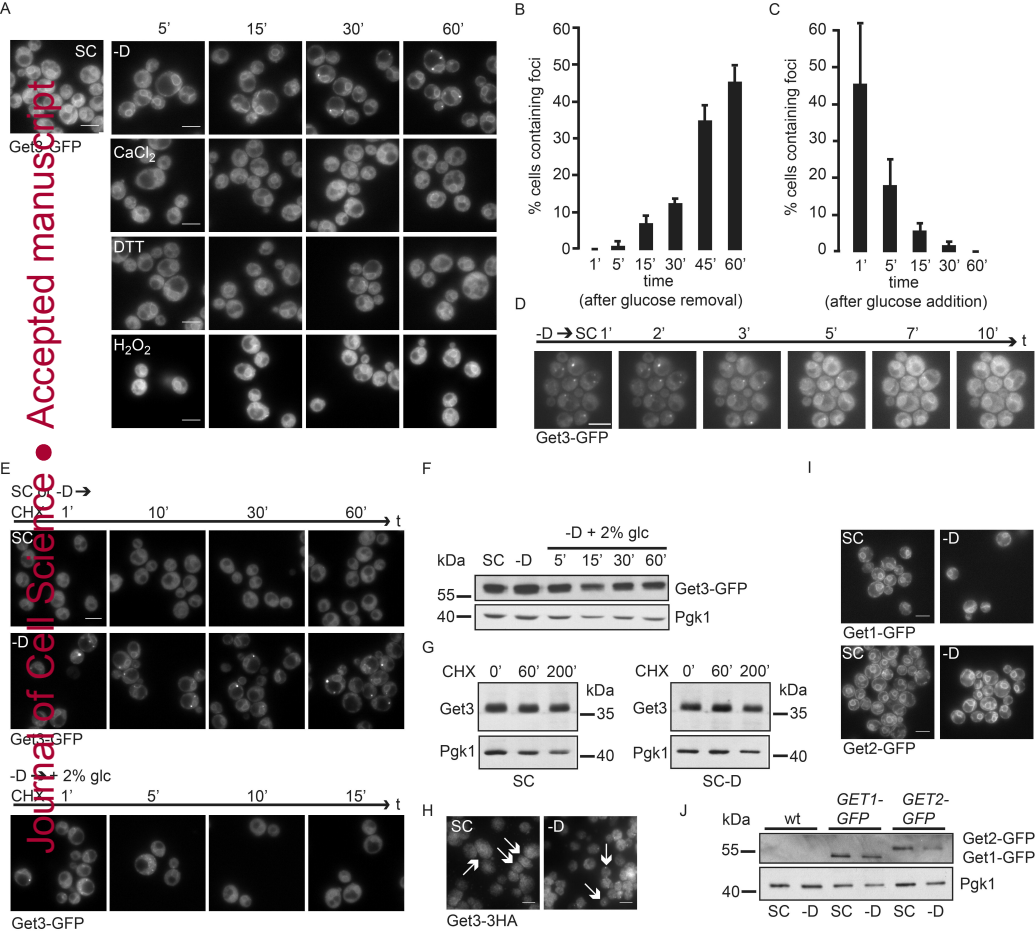

Figure 2